Tetrahedron 67 (2011) 1468–1478

Contents lists available at ScienceDirect

Tetrahedron

journal homepage: www.elsevier.com/locate/tet

Spectroscopic, semi-empirical and antimicrobial studies of a new amide of monensin A with 4-aminobenzo-15-crown-5 and its complexes with Na^+ cation at 1:1 and 1:2 ratios

Daniel Łowicki [a], Adam Huczyński [a,*], Joanna Stefańska [b], Bogumil Brzezinski [a,*]

[a] Adam Mickiewicz University, Faculty of Chemistry, Grunwaldzka 6, 60-780 Poznan, Poland
[b] Medical University of Warsaw, Department of Pharmaceutical Microbiology, Oczki 3, 02-007 Warsaw, Poland

ARTICLE INFO

Article history:
Received 27 August 2010
Received in revised form 18 November 2010
Accepted 13 December 2010
Available online 17 December 2010

Keywords:
Ionophores
Monensin A amide
Crown ether
Spectroscopy
Antimicrobial properties

ABSTRACT

A new amide of monensin A with 4-aminobenzo-15-crown-5 (M-AM3) was synthesised and its ability to form complexes with Na^+ cations was studied by ESIMS, ^1H, ^{13}C and ^{23}Na NMR, FTIR and PM5 semi-empirical methods. ESI mass spectrometry indicates that in the gas phase M-AM3 amide forms complexes of 1:1 and 1:2 stoichiometry with Na^+ cations. The formation of such complexes is also confirmed in the acetonitrile solution, in which the existence of equilibrium between two structures A and B is found, of which B structure is dominant. The structures of M-AM3 and its 1:1 and 1:2 complexes with Na^+ cations are stabilised by various intramolecular hydrogen bonds, which are discussed in detail. The in vitro biological tests have demonstrated that the new M-AM3 amide shows good activity towards some strains of Gram-positive bacteria (MIC 25–50 μg/ml).

1. Introduction

Monensin A is a naturally occurring ionophoric antibiotic isolated from *Streptomyces cinnamonensis*.[1] The isolation procedure for the first time was published by Honey and Hoehn in 1967.[2] This ionophore shows various antimicrobial and biological activity. Therefore, monensin A has been successfully used in veterinary medicine as a coccidiostatic drug to treat and prevent coccidiosis in poultry as well as a non-hormonal growth-promoting agent applied to stimulate the growth of ruminants.[3] The antibacterial properties of monensin A arise from its ability to coordinate metal cations inside the cavity of its molecule with particular selectivity to sodium cation. The hydrophobic exterior of the molecule allows sodium transport across cell membranes leading to death of Gram-positive bacteria.[4]

Crown ethers discovered by Pedersen in the middle of the 20th century, are a considerable part of supramolecular chemistry.[5] These particular ethers are examples of synthetic ionophores capable of making host–guest systems with metal cations. The molecule of monensin A, similarly to those of crown ethers, has the hydrophilic interior including some oxygen atoms, able to bind metal cations by dipole–ion interactions, whereas the hydrophobic exterior permits them to diffuse in the lipid bilayer.

Recently, we described the synthesis and structural studies of new monensin A amides with aniline and allylamine demonstrating the ability of these compounds to create 1:1 complexes with some monovalent metal cations and their substantial antimicrobial activity against Gram-positive bacteria.[6]

In this paper we synthesised a new amide of monensin A with 4-aminobenzo-15-crown-5 (M-AM3) and studied its complexation properties of sodium cations using ^1H, ^{13}C and ^{23}Na NMR, FTIR, ESIMS, as well as PM5 semi-empirical methods. This new amide possesses two hydrophilic sites able to coordinate metal cations in comparison to monensin A amides discussed previously, i.e., the crown ether moiety and the sphere of the monensin A molecule both showing high affinity to sodium cation because the cation diameter well matches the molecule cavity size.[7–12] Therefore, two questions arise, if the new amide is able to form a complex of 1:2 stoichiometry with sodium cations, and which of the two moieties can complex the first cation primarily. In this paper we try to answer these questions and we also report the microbiological activity of the newly synthesised amide M-AM3 against Gram-positive bacteria.

2. Results and discussion

The structures of monensin A and M-AM3 together with the atom numbering are shown in Scheme 1. The numbers of oxygen atoms are shown in brackets.

* Corresponding authors. Tel.: +48 61 829 1330; fax: +48 61 829 1505; e-mail addresses: adhucz@amu.edu.pl (A. Huczyński), bbrzez@amu.edu.pl (B. Brzezinski).

0040-4020/$ – see front matter © 2010 Elsevier Ltd. All rights reserved.
doi:10.1016/j.tet.2010.12.033

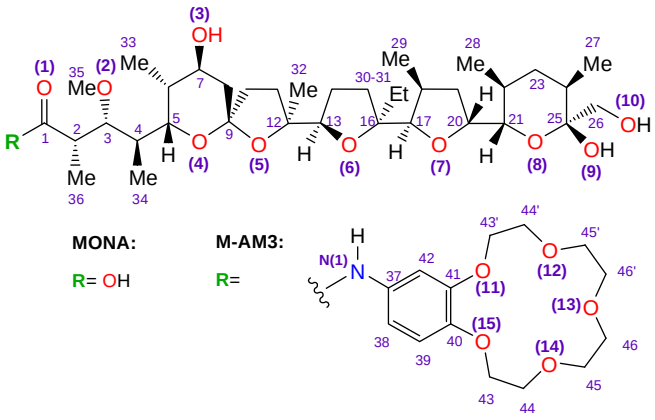

Scheme 1. The structures and atom numbering of MONA and M-AM3.

2.1. Synthesis

M-AM3 amide was synthesised in the reaction between the monensic acid (MONA) and 4-aminobenzo-15-crown-5 (AB15C5) in the presence of 1,3-dicyclohexylcarbodiimide (DCC) with the addition of 1-hydroxybenzotriazole (HOBt) as a catalyst (Scheme 2). This one-pot reaction led to M-AM3 obtained with 71% yield. It is interesting to note that without the addition of the HOBt catalyst, under the same reaction conditions, no expected amide was formed.

2.2. ^{1}H and ^{13}C NMR measurements

The ^{1}H and ^{13}C NMR data of M-AM3 and its 1:1 and 1:2 complexes with Na^{+} cations all in CD_3CN are shown in Tables 1 and 2, respectively. The ^{1}H and ^{13}C NMR signals were assigned using one- and two-dimensional (COSY, HETCOR, HMQC, HMBC and NOESY) spectra as well as by the ^{1}H NMR measurements with the addition of CD_3OD to the sample.

In the ^{1}H NMR spectra of M-AM3, its 1:1 and 1:2 complexes with Na^{+} cations (Table 1), the signals of the protons of all three OH and one NH groups are separate as illustrated in Fig. 1. The OH proton signals observed in the spectrum of M-AM3 at 4.07 ppm, 3.86 ppm, 2.75 ppm and 8.38 ppm are assigned to the O(3)H, O(9)H, O(10)H and N(1)H groups, respectively, whereas in the spectra of the complexes at 1:1 and 1:2 ratio the O(9)H and O(10)H proton signals are shifted to higher frequencies suggesting various involvement of these groups in formation of hydrogen bonds within the complexes.

A comparison of the ^{13}C NMR chemical shifts in the spectra of the complexes with those observed in the spectrum of M-AM3 reveals (Table 2) that not only the chemical shifts of the carbon atoms neighbouring the oxygen atoms involved in the coordination of Na^{+} cation but also the chemical shifts of some carbon atoms from the lipophilic sphere are visibly changed.

These changes indicate that upon complexation also conformational modifications of the M-AM3 molecule skeleton occur. The most interesting results regarding to the complexation process are connected with the ^{13}C NMR chemical shifts of the crown ether moiety.

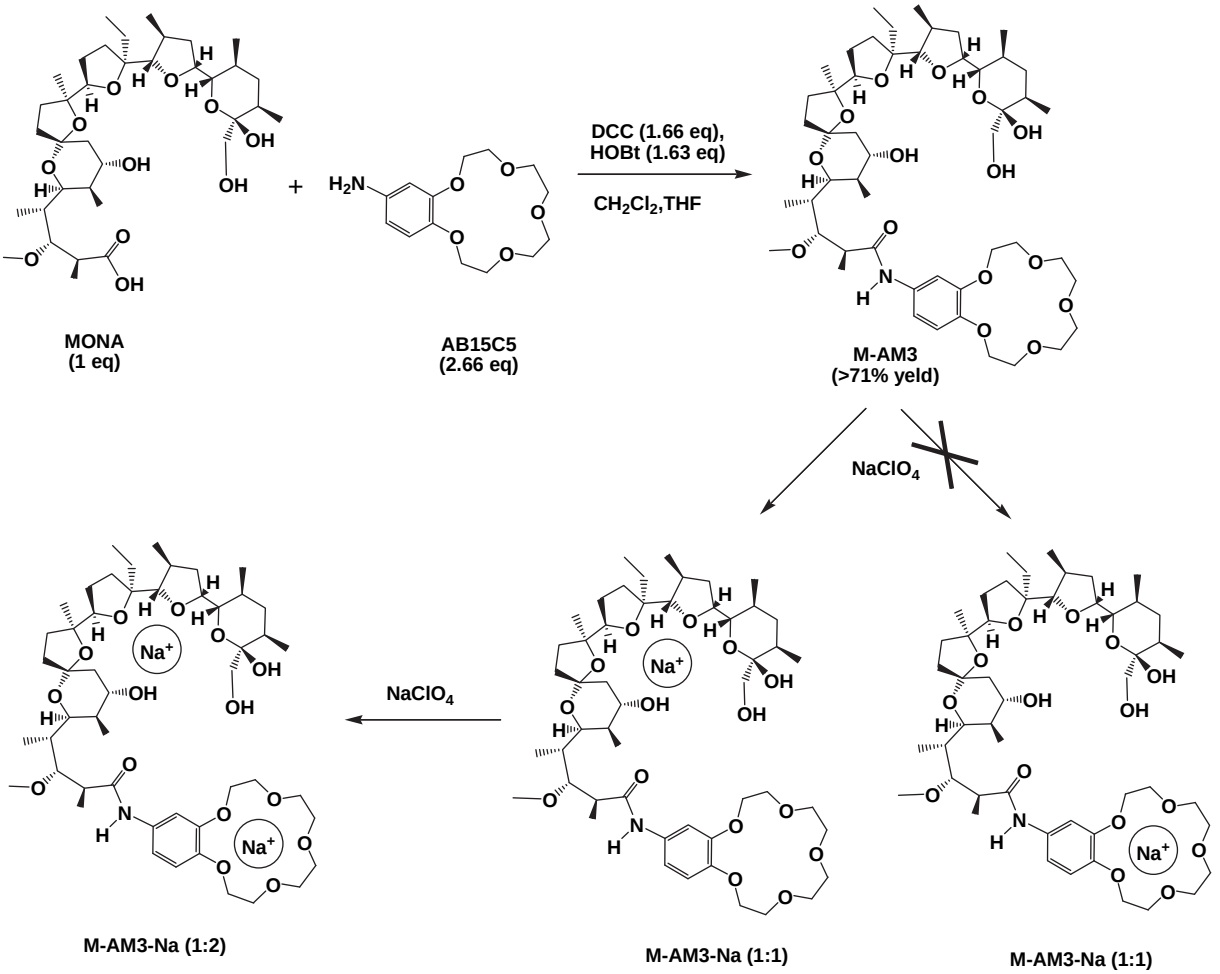

Scheme 2. The diagram of synthesis of M-AM3 and its complexes with sodium perchlorate.

Table 1
^{1}H NMR chemical shifts (ppm) of M-AM3 and its complexes with sodium perchlorate at 1:1 and 1:2 ratio measured in CD_3CN

No. atom	Chemical shifts (ppm)			Differences (Δ) between chemical shifts (ppm)	
	M-AM3	M-AM3–Na (1:1)	M-AM3–Na (1:2)	Δ1	Δ2
1	—	—	—	—	—
2	2.55	2.75	2.74	0.20	0.19
3	3.38	3.50	3.53	0.12	0.15
4	2.03	2.21	2.25	0.18	0.22
5	3.97	4.02	4.02	0.05	0.05
6	1.92	1.69	1.64	−0.23	−0.28
7	3.62	3.86	3.90	0.24	0.28
8A	1.52	1.60	1.63	0.08	0.11
8B	1.94	1.96	2.01	0.02	0.07
9	—	—	—	—	—
10A	1.84	1.80	1.82	−0.04	−0.02
10B	1.84	2.01	2.03	0.17	0.19
11A	1.66	1.84	1.83	0.18	0.17
11B	1.98	1.87	1.90	−0.11	−0.08
12	—	—	—	—	—
13	3.49	3.64	3.65	0.15	0.16
14A	1.33	1.49	1.53	0.16	0.20
14B	1.62	1.88	1.91	0.26	0.29
15A	1.45	1.46	1.50	0.01	0.05
15B	1.99	2.25	2.29	0.26	0.30
16	—	—	—	—	—
17	3.84	3.95	3.95	0.11	0.11
18	2.20	2.30	2.32	0.10	0.12
19A	1.50	1.58	1.65	0.08	0.15
19B	2.10	2.16	2.16	0.06	0.06
20	4.14	4.38	4.41	0.24	0.27
21	3.52	3.79	3.81	0.27	0.29
22	1.36	1.45	1.48	0.09	0.12
23A	1.27	1.43	1.42	0.16	0.15
23B	1.42	1.66	1.65	0.24	0.23
24	1.68	1.67	1.68	−0.01	0.00
25	—	—	—	—	—
26A	3.35	3.47	3.50	0.12	0.15
26B	3.35	3.73	3.78	0.38	0.43
27	0.88	0.86	0.88	−0.02	0.00
28	0.81	0.84	0.84	0.03	0.03
29	0.90	0.89	0.91	−0.01	0.01
30A	1.50	1.46	1.48	−0.04	−0.02
30B	1.50	1.65	1.71	0.15	0.21
31	0.88	0.90	0.92	0.02	0.04
32	1.39	1.44	1.49	0.05	0.10
33	0.89	0.88	0.87	−0.01	−0.02
34	1.02	1.05	1.05	0.03	0.03
35	3.36	3.46	3.48	0.10	0.12
36	1.20	1.30	1.33	0.10	0.13
37	—	—	—	—	—
38	6.98	7.07	7.00	0.09	0.02
39	6.81	6.91	7.11	0.10	0.30
40	—	—	—	—	—
41	—	—	—	—	—
42	7.51	7.36	7.36	−0.15	−0.15
43; 43′	4.01–4.03[a]	4.07–4.09[a]	4.12–4.16[a]	0.05–0.06	0.12–0.13
44; 44′	3.77–3.78[a]	3.79–3.81[a]	3.84–3.87[a]	0.02–0.03	0.07–0.09
45; 45′; 46; 46′	3.62–3.63[a]	3.64–3.67[a]	3.69–3.73[a]	0.02–0.04	0.07–0.10
N(1)H	8.38	8.60	8.43	0.22	0.05
O(3)H	4.07	4.06	3.86	−0.01	−0.21
O(9)H	3.86	6.12	5.92	2.26	2.06
O(10)H	2.75	3.76	4.19	1.01	1.44

$\Delta1=\delta_{\text{M-AM3–Na (1:1)}}-\delta_{\text{M-AM3}}$; $\Delta2=\delta_{\text{M-AM3–Na (1:2)}}-\delta_{\text{M-AM3}}$.
A,B—protons of methylene groups.
[a] overlapped signals (the approximate values).

In the spectrum of the 1:1 complex all, signals of the crown carbon atoms are slightly shifted towards lower ppm values. These shifts become significantly more pronounced in the spectrum of 1:2 complex, in which the crown ether moiety is fully complexed. Comparison of the ^{13}C NMR data of the 1:2 complex with those obtained for the 1:1 complex of AB15C5 with Na^+ cation (Table 3) confirmed this observation. Thus, on the basis of the ^{1}H and ^{13}C NMR measurements, in the 1:1 complex of M-AM3 with Na^+, this cation was concluded to be almost completely coordinated by the monensin moiety, although formation of a complex in which the crown ether moiety interacts, especially in an intermolecular manner, with the cation is also probable.

2.3. ^{23}Na NMR measurements

The ^{23}Na NMR spectra of acetonitrile-d_3 solutions of the 1:1 and 1:2 complexes of M-AM3 with Na^+ cations are compared with the spectra of AB15C5–Na complex, monensin A sodium salt (MON-Na)

Table 2
^{13}C NMR chemical shifts (ppm) of M-AM3 and its complexes with sodium perchlorate at 1:1 and 1:2 ratio measured in CD_3CN

No. atom	Chemical shifts (ppm)			Differences (Δ) between chemical shifts (ppm)	
	M-AM3	M-AM3–Na (1:1)	M-AM3–Na (1:2)	Δ1	Δ2
1	173.63	176.66	177.10	3.03	3.47
2	43.91	43.88	43.81	−0.03	−0.10
3	82.67	81.58	80.84	−1.09	−1.83
4	37.99	35.11	35.73	−2.88	−2.26
5	68.23	68.59	68.94	0.36	0.71
6	36.27	37.06	37.05	0.79	0.78
7	71.00	70.77	70.62	−0.23	−0.38
8	35.52	33.83	34.53	−1.69	−0.99
9	107.52	108.08	108.10	0.56	0.58
10	39.77	39.78	39.76	0.01	−0.01
11	32.67	32.38	33.26	−0.29	0.59
12	87.21	86.71	86.65	−0.50	−0.56
13	83.23	82.34	82.27	−0.89	−0.96
14	24.59	26.10	27.11	1.51	2.52
15	31.61	30.70	32.21	−0.91	0.60
16	88.28	87.08	86.92	−1.20	−1.36
17	86.07	85.50	85.51	−0.57	−0.56
18	35.65	34.57	35.03	−1.08	−0.62
19	35.41	33.21	33.74	−2.20	−1.67
20	78.45	76.95	76.89	−1.50	−1.56
21	77.56	76.13	75.95	−1.43	−1.61
22	34.62	31.53	30.65	−3.09	−3.97
23	37.77	35.13	35.97	−2.64	−1.80
24	34.89	36.21	36.88	1.32	1.99
25	97.97	98.75	98.81	0.78	0.84
26	67.35	67.10	67.05	−0.25	−0.30
27	18.09	16.28	16.16	−1.81	−1.93
28	16.49	16.83	16.73	0.34	0.24
29	16.08	14.40	14.26	−1.68	−1.82
30	30.15	30.15	30.20	0.00	0.05
31	8.36	8.13	8.12	−0.23	−0.24
32	28.56	27.20	28.37	−1.36	−0.19
33	11.30	10.55	10.55	−0.75	−0.75
34	12.30	13.19	13.11	0.89	0.81
35	58.62	58.29	57.94	−0.33	−0.68
36	15.35	14.58	14.12	−0.77	−1.23
37	134.08	133.47	133.67	−0.61	−0.41
38	112.83	114.29	114.81	1.46	1.98
39	115.20	114.91	115.07	−0.29	−0.13
40	146.00	145.55	144.65	−0.45	−1.35
41	149.85	148.83	147.86	−1.02	−1.99
42	108.11	108.53	108.56	0.42	0.45
43	69.40[a]	68.77[a]	68.03[a]	−0.63	−1.37
43′	70.14[a]	69.20[a]	68.71[a]	−0.94	−1.43
44	69.96[a]	69.39[a]	68.44[a]	−0.57	−1.52
44′	69.96[a]	69.39[a]	68.61[a]	−0.57	−1.35
45	71.36[a]	70.40[a]	69.34[a]	−0.96	−2.02
45′	71.43[a]	70.45[a]	69.42[a]	−0.98	−2.01
46	70.86[a]	69.83[a]	68.78[a]	−1.03	−2.08
46′	71.00[a]	69.93[a]	68.85[a]	−1.70	−2.15

$\Delta 1=\delta_{\text{M-AM3–Na (1:1)}}-\delta_{\text{M-AM3}}$; $\Delta 2=\delta_{\text{M-AM3–Na (1:2)}}-\delta_{\text{M-AM3}}$.
[a] —assignment may be reversed.

and pure $NaClO_4$ salt in Fig. 2. The ^{23}Na NMR data and the linewidths of the signals are collected in Table 4. All peaks were resonated at higher field region than the signal of NaCl as an external reference.

The ^{23}Na NMR spectrum of $NaClO_4$ shows one very sharp signal at −6.27 ppm. If Na^+ cation is complexed by the AB15C5 molecule a new signal at −3.68 ppm arises and it becomes slightly broadened. In the ^{23}Na NMR spectrum of MON-Na the signal of the complexed cation appears at about 0 ppm and it is significantly broader than those in the respective spectra of the $NaClO_4$ salt and the AB15C5–Na complex. A new signal is found in the spectrum of 1:1 complex of M-AM3–Na. This signal is observed at −1.15 ppm and it is strongly broadened. Surprisingly, in the ^{23}Na NMR spectrum of 1:2 complex two signals characteristic of complexed Na^+ cations separately in monensin and crown ether moieties are observed. These results clearly show that in the solution the first Na^+ cation is bonded by the monensin moiety of the M-AM3 molecule.

2.4. FTIR studies

In Fig. 3 the FTIR spectrum of M-AM3 (solid black line) is compared with the spectra of its 1:1 and 1:2 complexes with Na^+ cations, all recorded in acetonitrile solution. The regions of the ν(OH, NH) and ν(C=O) vibrations in an expanded scale are also shown in Fig. 3b and c, respectively. These figures show that the spectral features of the 1:1 and 1:2 complexes are very similar and significantly different than that of pure M-AM3 amide. These spectral similarities clearly demonstrate that in the 1:1 complex the Na^+ cation is complexed by the monensin moiety of the M-AM3 molecule.

Most characteristic, in the FTIR spectrum of M-AM3 are the bands assigned to the ν(OH) vibrations of the O(3)H, O(9)H and O(10)H groups with a maximum at ca. 3511 cm^{-1} and the ν(NH) vibrations of the N(1)H group at 3352 cm^{-1} (Fig. 3b), as well as the band assigned to the ν(C=O) vibrations arising at 1681 cm^{-1} (Fig. 3c). In the spectra of the 1:1 (red dotted line) and 1:2 (blue dashed line) complexes of M-AM3 with Na^+ (Fig. 3b) the bands assigned to the ν(OH) vibrations become more intense and more broadened with maxima at 3457 cm^{-1} and 3243 cm^{-1}. The first band is assigned to stretching vibrations of O(3)H and O(10)H groups and the second one to the O(9)H group. This indicates that in the structure of M-AM3–Na complexes the hydrogen bonds of O(9)H group become clearly stronger when compared to that in the uncomplexed M-AM3 molecule. Such interpretation is consistent with the ^{1}H NMR data (Table 1 and Fig. 1).

The position of the band assigned to the ν(NH) vibrations of the N(1)H amide group is independent of the complexation process and is always observed at ca. 3352 cm^{-1}. This observation is also in good agreement with the ^{1}H NMR data, because the N(1)H proton signal in the respective spectra of M-AM3 and its cation complexes is found between 8.38 and 8.60 ppm.

The amide I and amide II bands in the FTIR spectrum of M-AM3 are observed at 1681 cm^{-1} and 1532 cm^{-1}, respectively (Fig. 3c). The spectral feature of these bands changes strongly with formation of complexes with Na^+ cations but these changes are independent of the stoichiometric ratio. In the spectra of the 1:1 and 1:2 M-AM3 complexes with Na^+, instead of only one amide I band, two bands at 1677 cm^{-1} and 1656 cm^{-1} are observed indicating the existence of an equilibrium between the complexes in which the oxygen atom of amide group takes part in the complexation process or not, i.e., two types of complexes exist in acetonitrile. The absorptions of these amide I bands indicate that the concentration of the complexes in which the carbonyl group is involved in the coordination process is predominant. A hypothetical equilibrium between the complexed and the ligand-free form can be excluded on the basis of the NMR data, since none of the ^{1}H NMR spectra of the complexes (Fig. 1) exhibit the O(10)H signal at 2.75 ppm, typical of uncomplexed M-AM3.

2.5. Electrospray mass spectrometry (ESIMS) measurements

High resolution mass spectrometry with the use of electrospray is an excellent method for investigation of host–guest systems, especially organic ligands with organic as well as inorganic cations.

The main m/z signals in the ESIMS spectra of the 1:1 and 1:2 mixtures of M-AM3 with the Na^+ cations at various cone voltages are collected in Table 5 (the respective spectra are shown in Figs. S1 and S2 in Supplementary data). According to these data, M-AM3 is able to form the complexes with sodium cations of 1:1 and 1:2 stoichiometry, respectively.

The ESIMS spectra of the 1:1 mixture of M-AM3 with the Na^+ cations in the region of cv=10–70 V show only one signal at

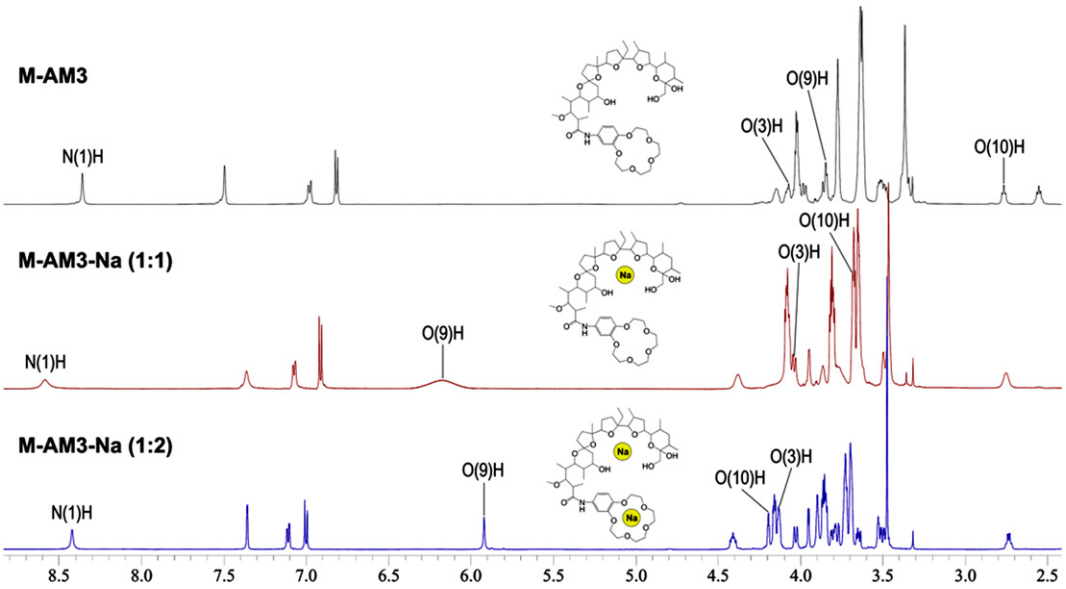

Fig. 1. ^{1}H NMR in region of OH and NH proton signals of: M-AM3, M-AM3–Na (1:1) and M-AM3–Na (1:2) measured in CD_3CN.

Table 3
^{13}C NMR chemical shifts (ppm) of AB15C5 and its 1:1 complex with sodium perchlorate measured in CD_3CN

No. atom	AB15C5 (ppm)	AB15C5–Na (ppm)	Δ1 ppm
37	141.62	139.43	−2.19
38	106.98	107.69	0.71
39	118.02	117.60	−0.42
40	144.14	145.15	1.01
41	151.15	149.20	−1.95
42	102.41	101.55	−0.86
43	70.43[a]	68.65[a]	−1.78
43′	70.79[a]	68.85[a]	−1.94
44	68.97[a]	67.44[a]	−1.53
44′	69.98[a]	68.59[a]	−1.39
45	71.23[a]	69.33[a]	−1.90
45′	71.38[a]	70.18[a]	−1.20
46	71.15[a]	68.97[a]	−2.18
46′	71.18[a]	69.06[a]	−2.12

$\Delta 1 = \delta_{AB15C5-Na} - \delta_{AB15C5}$.
[a] —assignment may be reversed.

m/z=959 indicating the formation of exclusively one type of complex, that of 1:1 stoichiometry. With increasing cone voltage values above 70 V the relative intensity of the signal of the 1:1 complex decreases and some new peaks of fragment ions appear. In the respective spectra of 1:2 mixture only one signal at m/z=491 of the 1:2 stoichiometry complex is found in the range of cv=10–50 V. At cv=70 V, additionally to the peak characteristic of the 1:2 complex, the one testifying the formation of the 1:1 complex (at m/z=959) and peaks of some other fragment ions are observed. With further increase in the cone voltage, the signals of the 1:1 and 1:2 complexes almost vanish and instead, only signals of various fragment cations are observed. The proposed fragmentation pathways for 1:1 and 1:2 complexes based on analysis of the fragment ions are illustrated in Schemes 3 and 4, respectively.

The differences in the fragmentation of the 1:1 and 1:2 complexes are detected by comparing the relative intensity of the signals at m/z=462, 390 and 332 and partially that at m/z=474. All these signals are dominant in the spectra of both complexes and are assigned to the fragment cations including the crown ether moiety although their relative intensity increases much stronger at the same cv values in the spectra of 1:2 complex. In contrast, in the spectra of both complexes the signals of the fragment cations including monensin moiety play only marginal role.

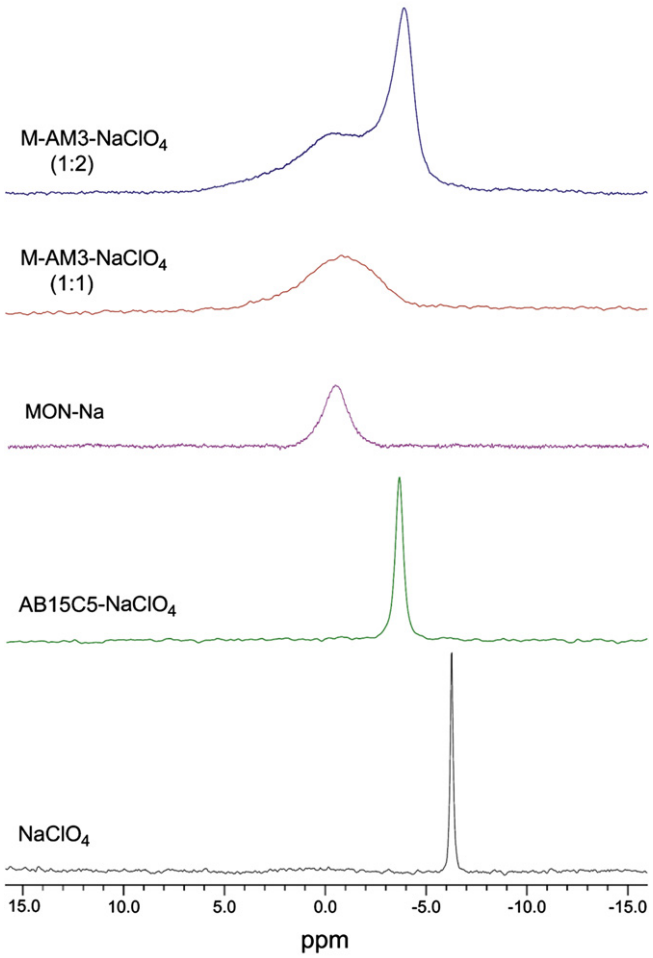

Fig. 2. ^{23}Na NMR spectra of $NaClO_4$ [black line], AB15C5–$NaClO_4$ complex [green line], MON-Na sodium salt [violet line] as well as M-AM3–$NaClO_4$ complexes at 1:1 [red line] and 1:2 [blue line] ratios, respectively measured in CD_3CN (An external reference—1 mol dm^{-3} NaCl).

Table 4
^{23}Na NMR chemical shifts: δ (ppm) and line widths: $\Delta\nu^{1/2}$ (Hz) in CD_3CN (an external reference: 1 mol dm^{-3} NaCl)

Compound	δ (ppm)	$\Delta\nu^{1/2}$ (Hz)
$NaClO_4$	−6.27	10
AB15C5–Na	−3.68	45
MON-Na	−0.05[a]	270
M-AM3–Na (1:1)	−1.15[a]	650
M-AM3–Na (1:2)	−0.40[a]	720
	−4.00	210

[a] Broad signal.

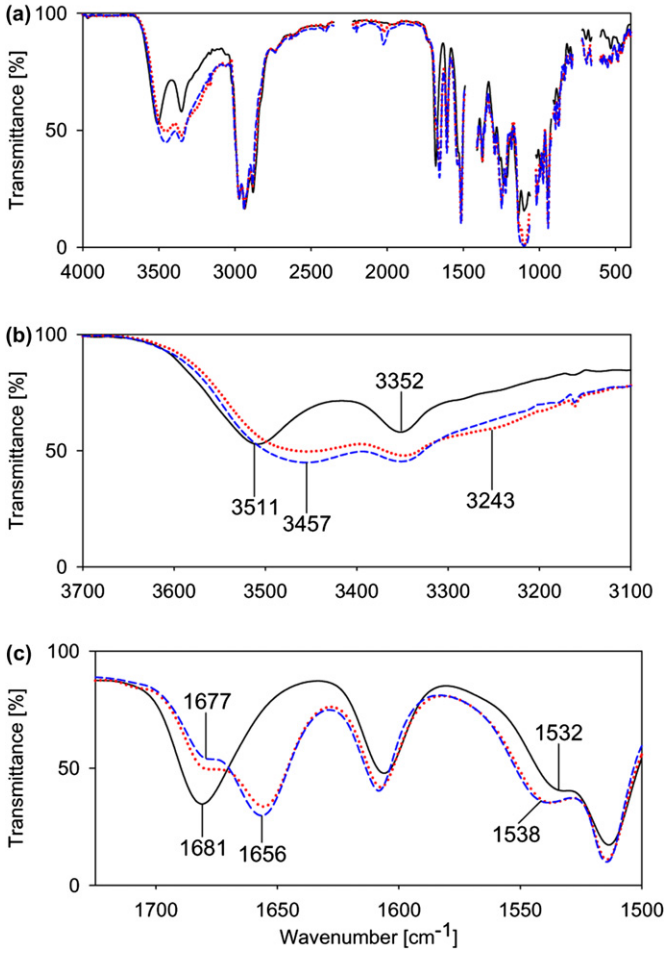

Fig. 3. FTIR spectra of: M-AM3 [solid black line], M-AM3–Na (1:1) [red dotted line] and M-AM3–Na (1:2) [blue dashed line] in the ranges of: (a) MIR 4000-400 cm^{-1}, (b) ν (OH,NH) 3700–3100 cm^{-1}, (c) ν(C=O) 1800-1500 cm^{-1} stretching vibrations recorded in CH_3CN.

In conclusion, the formation of stable 1:1 and 1:2 complexes between the M-AM3 and Na^+ cations in the gas phase can be evidenced by the ESIMS method. The complex of the 1:1 stoichiometry seems to be more stable than that of 1:2 stoichiometry, because the first one can be formed from the 1:2 complex and its fragmentation starts at higher *cv* values. Furthermore, if the fragmentation of the complexes takes place, the fragments including the benzocrown parts show much higher affinity to Na^+ cations than the monensin fragment.

2.6. Semi-empirical calculations

On the basis of the spectroscopic results, the heats of formation (HOF) of the structures of M-AM3 and its 1:1 and 1:2 complexes with Na^+ cations were calculated (Table 6) using PM5 semi-empirical method. The structures of M-AM3 and its sodium complexes at the 1:1 and 1:2 ratio involving both types: A—structure in which the C=O group does not participate in complexation process and B—structure in which the C=O group takes part in the coordination process, are visualised in Figs. S3–S7 in Supplementary data. The hydrogen and the coordination bonds in these structures are marked by dots. The ΔHOF values show that the structures of M-AM3 with Na^+ cations (ratios 1:1 and 1:2) in which the carbonyl group is involved in the complexation process (type B) are energetically more favourable than those in which the carbonyl group is not involved in this process (type A), but the existence of these both types of complexes is possible. For the complex of 1:1 stoichiometry in which the Na^+ cation is located in crown ether cavity (Type C, Table 6) the gain of energy during the complexation process is the lowest ΔHOF=−98.71 kcal/mol, which clearly confirms that this structure is totally unfavourable. The ΔHOF values for both A and B types of the 1:2 complex are only limited higher than those of the 1:1 complexes and much smaller than the respective sum of A+C and B+C types obtained for the formation of the 1:1 complexes. This result means that both A and B types of the 1:2 complex are energetically slightly more favourable than the respective structures of the 1:1 complex.

The interatomic distances between the oxygen atoms of the most favoured calculated complexes of M-AM3 with the Na^+ cations and the partial charges at these atoms are given in Table 7. Analysis of these values shows that in the 1:1 and 1:2 complexes some oxygen atoms of the monensin moiety, such as O(1), O(3), O(5), O(6), O(7), O(8) and O(10) are involved in the coordination of the Na(1) sodium cation, whereas in the complex of 1:2 stoichiometry all the oxygen atoms of the crown ether moiety are also involved in the complexation of the second sodium cation, i.e., Na(2).

The partial charges of both sodium cations in the 1:2 complex of M-AM3–Na, i.e., Na(1)=+0.297 located in the monensin part and

Table 5
The main peaks in the ESI mass spectra of the 1:1 and 1:2 complexes of M-AM3 with Na^+ cations at various cone voltages

Complex	Cone voltage [V]	Main *m/z* peaks (relative intensities [%])
M-AM3–Na (1:1)	10	959 (*100*)
	30	959 (*100*)
	50	959 (*100*)
	70	959 (*100*),
	90	959 (*100*), 479 (*5*), 462 (*15*), 461 (*10*), 390 (*12*), 332 (*10*)
	110	959 (*100*), 941 (*10*), 507 (*10*), 501 (*10*), 479 (*15*), 474 (*23*), 462 (*35*), 461 (*20*), 443 (*5*), 390 (*8*), 332 (*8*)
	130	959 (*21*), 941 (*5*), 507 (*18*), 501 (*30*), 483 (*11*), 479 (*20*), 474 (*30*), 462 (*100*), 461 (*21*), 443 (*5*), 390 (*28*), 332 (*17*)
M-AM3–Na (1:2)	10	491 (*100*)
	30	491 (*100*)
	50	491 (*100*), 482 (*10*)
	70	959 (*50*), 507 (*20*), 501 (*32*), 491 (*100*), 483 (*60*), 474 (*60*), 462 (*78*), 461 (*30*), 443 (*10*), 390 (*27*), 332 (*13*)
	90	959 (*45*), 507 (*10*), 501 (*18*), 491 (*15*), 483 (*5*), 479 (*15*), 474 (*45*), 462 (*73*), 461 (*30*), 443 (*12*), 390 (*100*), 332 (*62*)
	110	959 (*60*), 941 (*3*), 507 (*12*), 501 (*18*), 491 (*13*), 483 (*5*), 479 (*18*), 474 (*30*), 462 (*72*), 461 (*35*), 443 (*10*), 390 (*74*), 332 (*100*)
	130	959 (*15*), 941 (*2*), 507 (*17*), 501 (*30*), 491 (*10*), 483 (*2*), 479 (*25*), 474 (*35*), 462 (*100*), 461 (*30*), 443 (*5*), 390 (*43*), 332 (*32*)

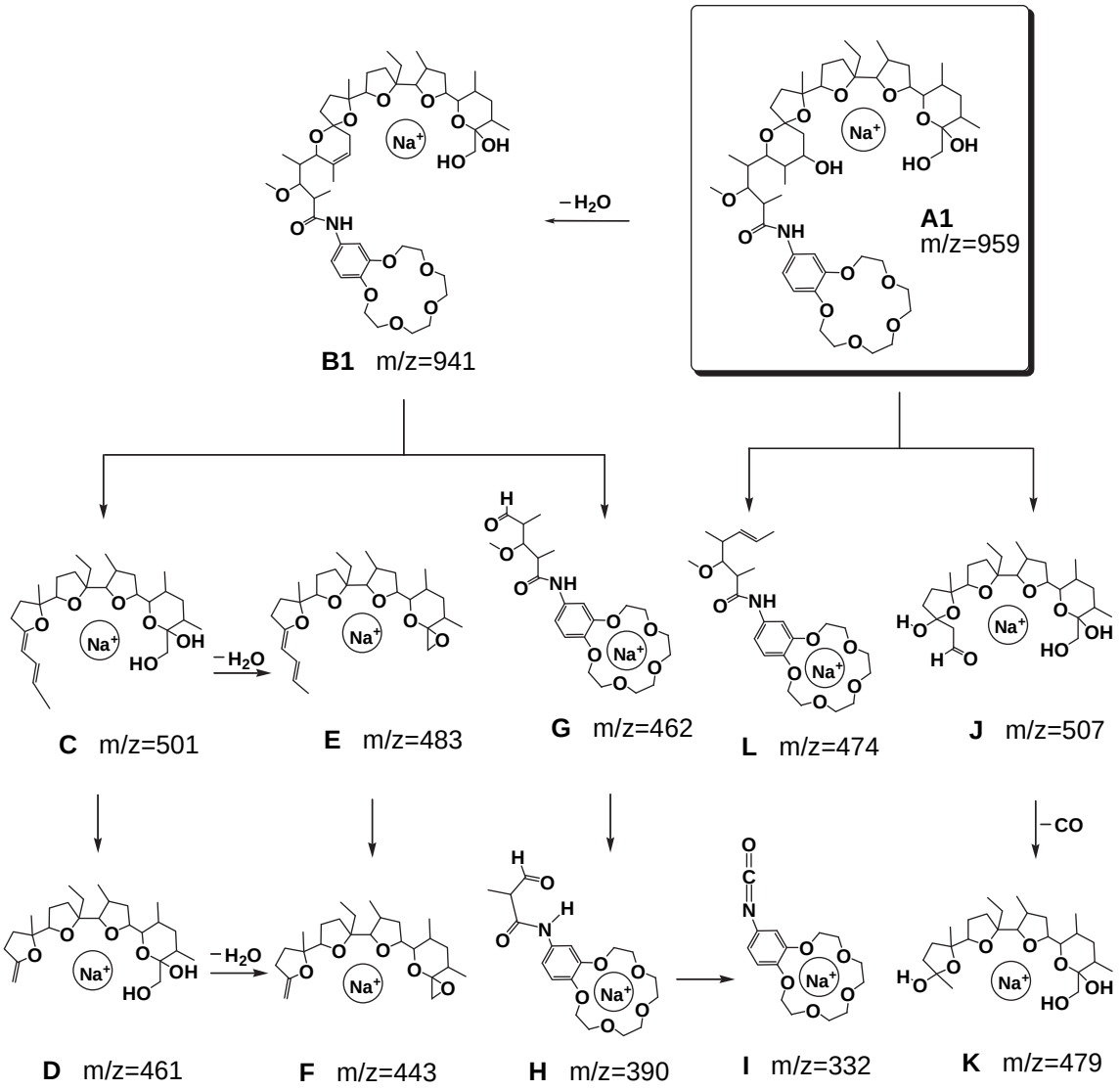

Scheme 3. The proposed fragmentation pathways of M-AM3 complex with Na^+ cation in 1:1 ratio.

Na(2)=+0.580 placed in the crown ether part, can also explain different linewidths of the respective signals in the ^{23}Na NMR spectra of this complex.

The calculated lengths and angles of the hydrogen bonds in which the OH groups are engaged are summarized in Table 8. In the calculated structure of M-AM3 (Fig. S3, Supplementary data) all three OH groups and one NH group are involved in intramolecular hydrogen bonds. Two of them, i.e., O(9)H and O(10)H are engaged in the intramolecular hydrogen bonds with the O(1) oxygen atom of the C=O amide group. With formation of the 1:1 and 1:2 complexes of type B between M-AM3 and Na^+ cations (Figs S5, S7; Supplementary data) these hydrogen bonds get broken because the O(1) oxygen atom is involved in the coordination process. For this reason the signal of the C(1) carbon atom in the ^{13}C NMR spectra of the complexes is shifted towards higher ppm values in comparison with its position in the spectrum of M-AM3 (Table 2). In the structures of the complexes a new bifurcated hydrogen bond with participation of the O(9)H and O(10)H groups and O(2) oxygen atom is created. This observation can also explain the shift of the ^1H NMR proton signal of the C(35) methyl group in both 1:1 and 1:2 M-AM3–Na complexes in relation to the position of this signal in M-AM3.

In the A type structure of the 1:1 and 1:2 M-AM3–Na complexes, the C=O carbonyl group is not involved in the coordination process of the sodium cation or in any hydrogen bond (Figs S6, S8; Supplementary data). In this structure a new bifurcated hydrogen bond between the O(2) atom and two O(9)H and O(10)H groups is however conserved.

The O(3)H hydroxyl group in the M-AM3 molecule is involved in a hydrogen bond with O(8) oxygen atom, whereas in all calculated complex structures this hydroxyl group is hydrogen bonded to the O(7) oxygen atom.

2.7. Antimicrobial activity

In this study we also wanted to determine the antimicrobial activity of the new amide M-AM3 composed of natural and synthetic ionophores.

Monensin A (MONA) and its amide (M-AM3) were tested in vitro for their antibacterial and antifungal activity. The micro-organisms used in this study were as follows: Gram-positive bacteria, Gram-negative rods and yeasts. Monensin A and M-AM3 were exclusively active against Gram-positive bacteria. For Gram-negative micro-organisms tested no activity was detected. This result was

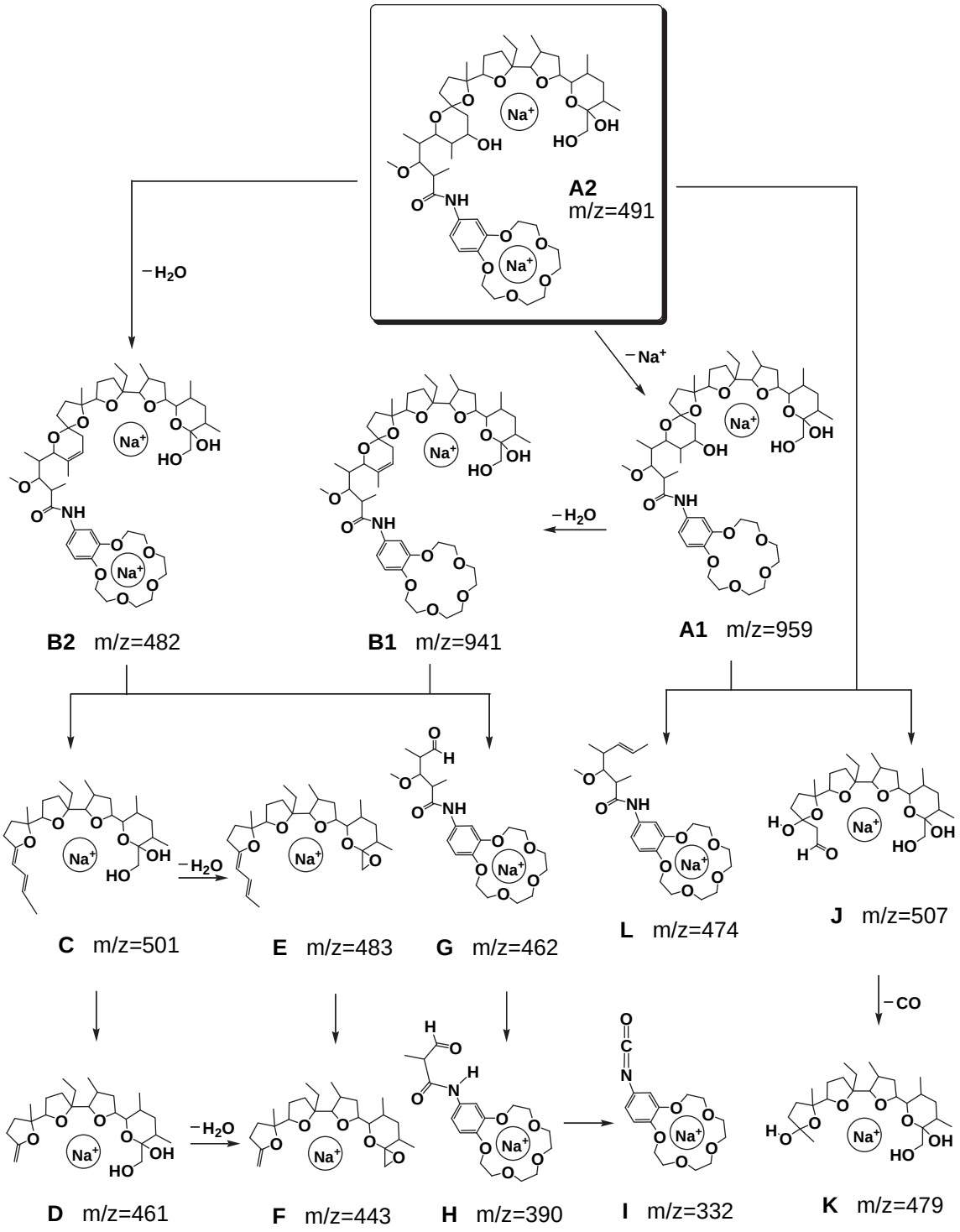

Scheme 4. The proposed fragmentation pathways of M-AM3 complex with Na^+ cations in 1:2 ratio.

expected because the cell walls of Gram-negative bacteria do not permit penetration of hydrophobic molecules of high molecular weights and thus the micro-organisms are not susceptible to the action of monensin and its M-AM3 derivative. Furthermore, Monensin A and M-AM3 are also inactive against strains *Candida* (*C. albicans* and *C. parapsilosis*). The antimicrobial properties of both MONA and M-AM3 are expressed by the minimum inhibitory concentration (MIC) as well as by the growth inhibition zone (Giz) and presented in Table 9. M-AM3 shows appreciable activity towards some human pathogenic bacteria (Giz 12–17 mm; MIC 25–50 μg/ml).

The spectroscopic and structural studies of the crown ether amide derivative of monensin A (M-AM3) show that this compound is able to form 1:1 as well as 1:2 complexes with sodium cation, while the parent antibiotic molecule forms with sodium cation exclusively the complex of 1:1 stoichiometry. Chemical modification of monensin A changes not only the stoichiometry of the complex, but also the type of the cation transport by this antibiotic. Monensin A

Table 6
Heat of formation (kcal/mol) of M-AM3 and its 1:1 and 1:2 complexes with the Na^+ cations calculated by PM5 method (WinMopac 2003)

Compound	HOF (kcal/mol)[a]	ΔHOF (kcal/mol)[a]
M-AM3	−594.29	
M-AM3+Na^+ (1:1)$_{uncomplexed}$ (A)	−452.23	−200.66
M-AM3+Na^+ (1:1)$_{complexed}$ (A)	−652.89	
M-AM3+Na^+ (1:1)$_{uncomplexed}$ (B)	−452.23	−221.28
M-AM3+Na^+ (1:1)$_{complexed}$ (B)	−673.51	
M-AM3+Na^+ (1:1)$_{uncomplexed}$ (C)	−452.23	−98.71
M-AM3+Na^+ (1:1)$_{complexed}$ (C)	−550.94	
M-AM3+2Na^+ (1:2)$_{uncomplexed}$ (A)	−310.17	−235.03
M-AM3+2Na^+ (1:2)$_{complexed}$ (A)	−545.20	
M-AM3+2Na^+ (1:2)$_{uncomplexed}$ (B)	−310.17	−240.77
M-AM3+2Na^+ (1:2)$_{complexed}$ (B)	−550.94	

ΔHOF=$HOF_{M\text{-}AM3+M\ complexed}$−$HOF_{M\text{-}AM3+M\ uncomplexed}$, M—sodium cation.
(A)—structure of M-AM3–Na complexes in which the C=O group is not involved in coordination of Na^+ cation.
(B)—structure of M-AM3–Na complex in which the C=O group is involved in coordination of Na^+ cation.
(C)—structure of M-AM3–Na (1:1) complex in which the Na^+ cation is coordinated by crown ether oxygen atoms.
[a] 1 kcal=4.167 kJ

Table 7
The interatomic distances (Å) and partial charges for O atoms of M-AM3 and coordinated cation in the most favoured calculated complexes by PM5 method (WinMopac 2003)

Complex with monovalent cation (types B)	Sodium cation partial charge	Coordinating bond	Coordinating oxygen atom partial charge	Distance (Å) coordinating atom→cation
M-AM3–Na (1:1)	+0.309	Na–O(1)	−0.417	2.41
		Na–O(3)	−0.417	2.40
		Na–O(5)	−0.380	2.36
		Na–O(6)	−0.357	2.39
		Na–O(7)	−0.370	2.36
		Na–O(8)	−0.354	2.39
		Na–O(10)	−0.377	2.41
M-AM3–Na (1:2)	+0.297 Na(1)	Na(1)–O(1)	−0.403	2.42
	+0.580 Na(2)	Na(1)–O(3)	−0.439	2.34
		Na(1)–O(5)	−0.382	2.39
		Na(1)–O(6)	−0.392	2.39
		Na(1)–O(7)	−0.366	2.34
		Na(1)–O(8)	−0.372	2.36
		Na(1)–O(10)	−0.405	2.42
		Na(2)–O(11)	−0.311	2.54
		Na(2)–O(12)	−0.358	2.48
		Na(2)–O(13)	−0.366	2.56
		Na(2)–O(14)	−0.356	2.48
		Na(2)–O(15)	−0.315	2.54

(Type B)—structure of M-AM3–Na complex in which the C=O group is involved in coordination of Na^+ cation.
Na(1)—sodium cation complexed by monensin moiety.
Na(2)—sodium cation complexed by crown ether moiety.

Table 8
The lengths (Å) and angles (°) of the hydrogen bonds for M-AM3 and its complexes in the most favoured calculated structures by PM5 method (WinMopac 2003)

Compound	Atoms engaged in hydrogen bonds	Length (Å)	Angle (°)
M-AM3	O(3)H···O(8)	2.75	126.5
	O(9)H···O(1)	2.71	121.3
	(10)H···O(1)–O	2.89	156.5
	N(1)H···O(2)	2.92	129.0
M-AM3–Na (1:1) (B type)	O(3)H···O(7)	2.58	105.6
	O(9)H···O(2)	2.92	148.2
	O(10)H···O(2)	2.97	146.2
M-AM3–Na (1:2) (B type)	O(3)H···O(7)	2.60	106.6
	O(9)H···O(2)	2.90	146.6
	O(10)H···O(2)	2.95	144.2

(B-type)—structure of M-AM3–Na complex in which the C=O group is involved in coordination of Na^+ cation.

Table 9
Antimicrobial activity of MONA and M-AM3: diameter of the growth inhibition zone [Giz, mm] and Minimal Inhibitory Concentration (MIC, μg/ml)

Tested strain	MONA		M-AM3	
	Giz (mm)	(MIC, μg/ml)	Giz (mm)	(MIC, μg/ml)
S. aureus NCTC 4163	22	2	14	50
S. aureus ATCC 25923	22	1	15	50
S. aureus ATCC 6538	20	2	14	50
S. aureus ATCC 29213	18	1	15	50
S. epidermidis ATCC 12228	15	2	12	50
B. subtilis ATCC 6633	22	1	15	50
B. cereus ATCC 11778	18	2	17	25
E. hirae ATCC 10541	—	12.5	—	400
M. luteus ATCC 9341	12	4	14	50
M. luteus ATCC 10240	12	2	15	50

—: Denotes lack of the growth inhibition zone.

forms the electroneutral complex with sodium (as monensin sodium salt) and its biological activity is connected with electroneutral exchange of the sodium cations and protons between extracellular and cytoplasmic sites of the bacterial membrane (as Na^+/H^+ antiporter).[13] However M-AM3 forms singly and doubly positively charged complexes, which cannot be transported across the membrane in the electroneural manner but rather in the electrogenic way.[4,14] It is also possible that the doubly charged complexes are too highly charged to be effectively incorporated into the cell membrane. The differences in the biological activities between monensin and M-AM3 can also be a result of the size and chemical nature of the substituent, which shows lipophilic character.

3. Conclusions

A new amide of monensin A (M-AM3) was synthesised in one-pot reaction in the yield of 71%. ESI mass spectrometry clearly confirms that the new M-AM3 amide forms complexes of 1:1 and 1:2 stoichiometry, which are stable up to about cv=70 V and 90 V, respectively. Fragmentation pathways for both complexes are proposed. The spectroscopic measurements indicate that the structures of the 1:1 and 1:2 complexes are stabilised by intramolecular hydrogen bonds in which all three hydroxyl groups of monensin A moiety are always involved. In the solution, the two structures: type A in which the O(1) oxygen atom of the C=O amide group does not participate in the complexation process and type B in which this oxygen atom is involved in the coordination process, are found to reach an equilibrium. At this equilibrium, independently of the complex stoichiometry, B type structure is dominant. The spectroscopic data and PM5 calculations indicate that in the 1:1 M-AM3–Na complex the sodium cation is localised in the monensin moiety and that the crown ether part plays no role in the coordination process. In vitro biological tests of M-AM3 amide carried out on various strains of Gram-positive and Gram-negative bacteria show its considerable activity against the G(+) strains used (Giz=12–17 mm; MIC= 25–50 μg ml^{-1}).

4. Experimental

4.1. General remarks

Monensin A sodium salt (MON-Na), 4-aminobenzo-15-crown-5 (AB15C5) as well as sodium perchlorate $NaClO_4$ were commercial products of Sigma and were used without any further purification. Because the sodium perchlorate was a hydrate, it was necessary to dehydrate it in several (6–10 times) evaporation steps from a 1:5 mixture of acetonitrile and absolute ethanol. The dehydration of the $NaClO_4$ hydrate was monitored by recording its FTIR spectrum in acetonitrile.

CH_3CN and CD_3CN spectral-grade solvents were stored over 3 Å molecular sieves for several days. All manipulations with the substances were performed in a carefully dried and CO_2-free glove box.

4.2. Preparation of monensin A amide with AB15C5 amine

Monensin A sodium salt (MON-Na) was dissolved in dichloromethane (CH_2Cl_2) and stirred vigorously with a layer of aqueous sulfuric acid (H_2SO_4; pH=1.5). The organic layer containing MONA was washed with distilled water, and dichloromethane was then evaporated under reduced pressure to dryness. A solution of MONA (1000 mg, 1.49 mmol), 1,3-dicyclohexylcarbodiimide (DCC—515 mg, 2.50 mmol) and 4-aminobenzo-15-crown-5 (AB15C5—1133 mg, 4.00 mmol) all dissolved in dichloromethane and 1-hydroxybenzotriazole (HOBt—330 mg, 2.44 mmol) dissolved in tetrahydrofuran was mixed together and stirred at a temperature between 0 and −10 °C for 24 h. After this time the reaction mixture was stirred at room temperature for the next 24 h, diluted with H_2O and extracted with CH_2Cl_2. The organic phase was evaporated under reduced pressure to dryness. The residue was suspended in hexane and filtered off to remove 1,3-dicyclohexylurea (DCU) as a by-product. The filtrate was evaporated under reduced pressure and purified by chromatography on silica gel (Fluka type 60) to give M-AM3 (988 mg, 71% yield) as an amorphous, brown solid.

Elemental analysis for M-AM3 ($C_{50}H_{81}NO_{15}$): Calculated: C 64.15%, H 8.72%, N 1.50%. Found: C 64.05%, H 8.78%, N 1.61%.

Furthermore, M-AM3 and its 1:1 and 1:2 complexes with sodium perchlorate were fully characterised by ESIMS, ^1H, ^{13}C NMR and FTIR spectroscopy.

4.3. Synthesis of 1:1 and 1:2 complexes of M-AM3 and 1:1 complex with AB15C5 with sodium cations

A 0.07 mol dm^{-3} solution of 1:1 complex of M-AM3 with sodium cation was obtained by adding equimolar amount of $NaClO_4$ dissolved in acetonitrile to acetonitrile solution of M-AM3.

A 0.07 mol dm^{-3} solution of 1:2 complex of M-AM3 with sodium cations was obtained by adding 2 equiv of $NaClO_4$ dissolved in acetonitrile to 1 equiv of M-AM3 dissolved in acetonitrile.

A 0.07 mol dm^{-3} solution of 1:1 complex of AB15C5 with sodium cation was obtained by adding equimolar amount of $NaClO_4$ dissolved in acetonitrile to acetonitrile solution of AB15C5.

The solvents were evaporated under reduced pressure to dryness and the residues were dissolved in an appropriate volume of dry CH_3CN and CD_3CN to obtain the respective complex of the 0.07 mol dm^{-3} concentration.

4.4. Spectroscopic measurements

The FTIR spectra of M-AM3 and its 1:1 and 1:2 complexes (0.07 mol dm^{-3}) with $NaClO_4$ were recorded in the mid infrared region in acetonitrile solutions using a Bruker IFS 113v spectrometer. A cell with Si windows and wedge-shaped layers was used to avoid interferences (mean layer thickness 170 μm). The spectra were taken with an IFS 113v FTIR spectrophotometer (Bruker, Karlsruhe) equipped with a DTGS detector; resolution 2 cm^{-1}, NSS=125. The Happ–Genzel apodization function was used. All manipulations with the compounds were performed in a carefully dried and CO_2-free glove box.

The ^1H and ^{13}C NMR spectra of M-AM3 and its 1:1 and 1:2 complexes (0.07 mol dm^{-3}) with $NaClO_4$ as well as AB15C5 and its 1:1 complex with $NaClO_4$ were recorded in CD_3CN solutions using Bruker Avance 600 MHz spectrometer. All spectra were locked to deuterium resonance of CD_3CN.

The ^1H NMR measurements were carried out at the operating frequency 600.0018 MHz, at temperature 293.0 K and using TMS as the internal standard. No window function or zero filling was used. The error of chemical shift value was 0.01 ppm.

^{13}C NMR spectra were recorded at the operating frequency 150.885 MHz, temperature 293.0 K and TMS as the internal standard. Line broadening parameters were 1 or 2 Hz. The error of chemical shift value was 0.1 ppm.

The ^1H and ^{13}C NMR signals were assigned independently for each species using one- or two-dimensional (COSY, HETCOR, HMQC, HMBC and NOESY) spectra.

^{23}Na NMR spectra of: $NaClO_4$, AB15C5–Na and M-AM3–Na (1:1) [concentration of $NaClO_4$=0.033 mol dm^{-3}], as well as M-AM3–Na (1:2) [concentration of $NaClO_4$=0.066 mol dm^{-3}] were recorded in CD_3CN solution. The operating frequency of Bruker Avance 600 MHz spectrometer was 158.71 MHz; spectral width *sw*=15,873 Hz; acquisition time at=2.0 s; spectral resolution HZpPT=0.48 Hz; *T*=293 K. The chemical shifts were measured with reference to 1 mol dm^{-3} aqueous solution of NaCl as an external standard.

4.5. ESIMS studies

The ESI (Electrospray ionisation) mass spectra were recorded on a Waters/Micromass (Manchester, UK) ZQ mass spectrometer equipped with a Harvard Apparatus syringe pump. All samples were prepared in acetonitrile. The samples of the 5×10^{-5} mol dm^{-3} concentrations being a solutions of 1:1 and 1:2 complexes of M-AM3 with Na^+ cations were infused into the ESI source using a Harvard pump at a flow rate of 20 μl min^{-1}. The ESI source potentials were: capillary 3 kV, lens 0.5 kV, extractor 4 V. The standard ESI mass spectra were recorded at the cone voltages: 10, 30, 50, 70, 90, 110 and 130 V. The source temperature was 120 °C and the desolvation temperature was 300 °C. Nitrogen was used as the nebulizing and desolvation gas at flow-rates of 100 and 300 dm^3 h^{-1}, respectively. Mass spectra were acquired in the positive ion detection mode with unit mass resolution at a step size of 1 *m*/*z* unit. The mass range for ESI experiments was from *m*/*z*=200 to 1000.

4.6. PM5 calculations

PM5 semi-empirical calculations were performed using the WinMopac 2003 program. In all cases, full geometry optimisation of M-AM3 and its complexes was carried out without any symmetry constraints.[15]

4.7. Microbiological analysis

The following micro-organisms were used in this study: *Gram-positive cocci*: *Staphylococcus aureus* NCTC 4163, *S. aureus* ATCC 25923, *S. aureus* ATCC 6538, *S. aureus* ATCC 29213, *Staphylococcus epidermidis* ATCC 12228, *Bacillus subtilis* ATCC 6633, *Bacillus cereus* ATCC 11778, *Enterococcus hirae* ATCC 10541, *Micrococcus luteus* ATCC 9341, *M. luteus* ATCC 10240; *Gram-negative rods*: *Escherichia coli* ATCC 10538, *E. coli* ATCC 25922, *E. coli* NCTC 8196, *Proteus vulgaris* NCTC 4635, *P. aeruginosa* ATCC 15442, *P. aeruginosa* NCTC 6749, *P. aeruginosa* ATCC 27863, *Bordetella bronchiseptica* ATCC 4617 and *yeasts*: *C. albicans* ATCC 10231, *C. albicans* ATCC 90028, *C. parapsilosis* ATCC 22019.

The micro-organisms used were obtained from the collection of the Department of Pharmaceutical Microbiology, Medical University of Warsaw, Poland.

Antimicrobial activity was examined by the disc-diffusion method under standard conditions using Mueller-Hinton II agar medium (Becton Dickinson) for bacteria and RPMI agar with 2% glucose (Sigma) according to CLSI (previously NCCLS) guidelines.[16]

Sterile filter paper discs (9 mm diameter, Whatman No 3 chromatography paper) were dripped with tested compound solutions (in MeOH or MeOH/DMSO 1:1) to load 400 μg of a given compound

per disc. Dry discs were placed on the surface of appropriate agar medium. The results (diameter of the growth inhibition zone) were read after 18 h of incubation at 35 °C. Compounds with recognised activity in disc-diffusion tests were examined by the agar dilution method to determine their MIC—Minimal Inhibitory Concentration (CLSI).[17] Concentrations of the agents tested in solid medium ranged from 3.125 to 400 μg ml^{-1}. The final inoculum of all studied organisms was 104 CFU ml^{-1} (colony forming units per ml), except the final inoculum for *E. hirae* ATCC 10541, which was 105 CFU ml^{-1}. Minimal inhibitory concentrations were read after 18 h of incubation at 35 °C.

Acknowledgements

D. Ł. wishes to thank the Adam Mickiewicz University Foundation in Poznan for fellowship.

Supplementary data

Supplementary data associated with this article can be found in online version at doi:10.1016/j.tet.2010.12.033.

References and notes

1. Agtarap, A.; Chamberlin, J. W.; Pinkerton, M.; Steinrauf, I. *J. Am. Chem. Soc.* **1967**, *89*, 5737–5739.
2. Honey, M. E.; Hoehn, M. M. *Antimicrob. Agents Chemother.* **1967**, *7*, 349–352.
3. (a) McEwen, S. A.; Fedorka-Cray, P. J. *Clin. Infect. Dis.* **2002**, *34*, S93–S106; (b) Shumard, R. F.; Callender, M. E. *Antimicrob. Agents Chemother.* **1967**, *7*, 369–377; (c) Butaye, P.; Devriese, L. A.; Haesebrouck, F. *Clin. Microbiol. Rev.* **2003**, *16*, 175–188; (d) Song, M. K.; Choi, S. H. *Asian–Australas. J. Anim. Sci.* **2001**, *14*, 123–135; (e) Salles, M. S. V.; De Sousa Lucci, C. *Rev. Bras. Zootec.* **2000**, *29*, 573–581; (f) Droumev, D. *Vet. Res. Commun.* **1983**, *7*, 85–99.
4. (a) Prabhananda, B. S.; Kombrabail, M. H. *Biochim. Biophys. Acta, Biomembr.* **1992**, *1106*, 171–177; (b) Nakazato, K.; Hatano, Y. *Biochim. Biophys. Acta* **1991**, *1064*, 103–110; (c) Mollenhauer, H. H.; Morre, D. J.; Rowe, L. D. *Biochim. Biophys. Acta* **1990**, *1031*, 225–246.
5. (a) Pedersen, C. J. *J. Am. Chem. Soc.* **1967**, *89*, 7017–7036; (b) Pedersen, C. J. *Angew. Chem., Int. Ed. Engl.* **1988**, *27*, 1021–1027; (c) Steed, J. W. *Coord. Chem. Rev.* **2001**, *215*, 171–221.
6. (a) Łowicki, D.; Huczyński, A.; Stefańska, J.; Brzezinski, B. *Eur. J. Med. Chem.* **2010**, *45*, 4050–4057; (b) Łowicki, D.; Huczyński, A.; Stefańska, J.; Brzezinski, B. *Tetrahedron* **2009**, *65*, 7730–7740; (c) Łowicki, D.; Huczyński, A.; Ratajczak-Sitarz, M.; Katrusiak, A.; Stefańska, J.; Brzezinski, B.; Bartl, F. *J. Mol. Struct.* **2009**, *923*, 53–59.
7. Cox, B. G.; Van Truong, N. *J. Chem. Soc., Faraday Trans. 1* **1984**, *80*, 3275–3284.
8. Huczyński, A.; Ratajczak-Sitarz, M.; Katrusiak, A.; Brzezinski, B. *J. Mol. Struct.* **2007**, *832*, 84–89.
9. Buschmann, H.-J.; Mutihac, R.-C.; Schollmeyer, E. *J. Solution Chem.* **2009**, *38*, 209–217.
10. Weber, E. *Ullmann's Encyclopaedia of Industrial Chemistry: Crown Ethers*; Wiley-VCH: Weinheim, 2007.
11. Huczyński, A.; Przybylski, P.; Brzezinski, B. *Tetrahedron* **2007**, *63*, 8831–8839.
12. Huczyński, A.; Przybylski, P.; Brzezinski, B.; Bartl, F. *Biopolymers* **2006**, *81*, 282–294.
13. (a) Pressmn, B. C. *Annu. Rev. Biochem.* **1976**, *45*, 501–530; (b) Sandeaux, R.; Sandeaux, J.; Gavach, C.; Brun, B. *Biochim. Biophys. Acta* **1982**, *684*, 127–132; (c) Riddell, F. G. *Chilarity* **2002**, *14*, 121–125; (d) Ben-Tal, N.; Sitkoff, D.; Bransburg-Zabary, S.; Nachliel, E.; Gutman, M. *Biochim. Biophys. Acta, Biomembr.* **2000**, *1466*, 221–233.
14. (a) Inabayashi, M.; Miyauchi, S.; Kamo, N.; Jin, T. *Biochemistry* **1995**, *34*, 3455–3460; (b) Tsukube, H.; Takagi, K.; Higashiyama, T.; Iwachido, T.; Hayama, N. *J. Chem. Soc., Chem. Commun.* **1986**, 448–449.
15. (a) Rocha, G. B.; Freire, R. O.; Simas, A. M.; Stewart, J. J. P. *J. Comput. Chem.* **2006**, *27*, 1101–1111; (b) Stewart, J. J. P. *Method J. Comput. Chem.* **1991**, *12*, 320–341; (c) Stewart, J. J. P. *J. Comput. -Aided Mater. Des.* **1990**, *4*, 1–103; (d) *CAChe 5.04 UserGuide*; Fujitsu: Beaverton, OR, USA, 2003.
16. Clinical and Laboratory Standards Institute *Performance Standards for Antimicrobial Disc Susceptibility Tests; Approved Standard M2-A9*; Clinical and Laboratory Standards Institute: Wayne, Pa, USA, 2006.
17. Clinical and Laboratory Standards Institute *Methods for Dilution Antimicrobial Susceptibility Tests for Bacteria That Grow Aerobically; Approved Standard M7-A7*; Clinical and Laboratory Standards Institute: Wayne, PA, USA, 2006.